NANO LETTERS

pubs.acs.org/NanoLett

Letter

Over 30-Fold Enhancement in DNA Translocation Dynamics through Nanoscale Pores Coated with an Anionic Surfactant

Neeraj Soni,[#] Navneet Chandra Verma,[#] Noam Talor, and Amit Meller*

Cite This: https://doi.org/10.1021/acs.nanolett.3c01096

Read Online

ACCESS | Metrics & More | Article Recommendations | Supporting Information

ABSTRACT: Solid-state nanopores (ssNPs) are single-molecule sensors capable of label-free quantification of different biomolecules, which have become highly versatile with the introduction of different surface treatments. By modulating the surface charges of the ssNP, the electro-osmotic flow (EOF) can be controlled in turn affecting the in-pore hydrodynamic forces. Herein, we demonstrate that negative charge surfactant coating to ssNPs generates EOF that slows-down DNA translocation speed by >30-fold, without deterioration of the NP noise, hence significantly improving its performances. Consequently, surfactant-coated ssNPs can be used to reliably sense short DNA fragments at high voltage bias. To shed light on the EOF phenomena inside planar ssNPs, we introduce visualization of the electrically neutral fluorescent molecule's flow, hence decoupling the electrophoretic from EOF forces. Finite elements simulations are then used to show that EOF is likely responsible for in-pore drag and size-selective capture rate. This study broadens ssNPs use for multianalyte sensing in a single device.

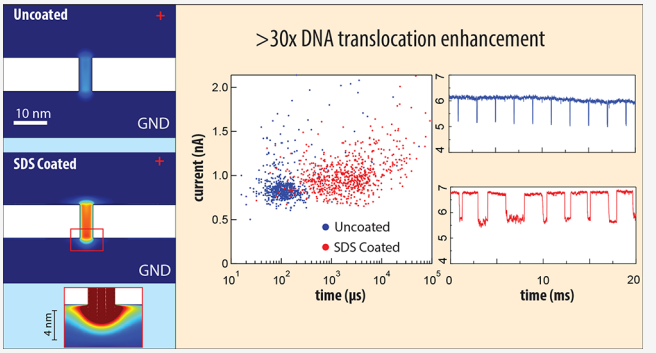

KEYWORDS: *Solid-state Nanopores, Single-molecule sensing, DNA translocation, Electroosmotic force, SDS-protein Complex, Voltage driven translocation*

Nanopores (NPs) are emerging single-molecule devices for label-free sensing of a broad range of analytes.[1−3] NPs use electrophoretic (EP) forces to focus and deliver biopolymers through a constriction made in a thin-membrane or a glass capillary narrowed to a nanoscale dimension.[3] The voltage-driven translocation dynamics of the analytes are governed by their in-pore friction, interactions with the device's interfaces, and polymer dynamics.[4] Additionally, electroosmotic flow (EOF) has been assumed to play critical roles in virtually all types of NPs, including protein pores, glass capillaries, as well as inorganic solid-state NPs.[5−8] The EOF, however, is often a double-edged sword role: liquid flow countering the EP motion may favorably slow down the translocation speed. But EOF extending outside the NP boundaries leads to repulsion of the analyte molecules away from the NP, hence unfavorably reducing their capture rate.[9]

The EOF phenomena has been extensively studied in glass capillaries,[10,11] but less is known about the EOF influence on molecular transport in the planar nanopore.[6,12] The in-pore EOF can be altered by manipulating its surface charge using organic coating or even light.[13,14] Recently, it has been shown that anionic surfactants, such as sodium dodecyl sulfate (SDS), facilitate single-file translocation of heat-denatured proteins even if these proteins are weakly or not charged at all in their native form,[15,16] opening potential avenues for single protein identification application. SDS-denatured proteins, however, are not ideal for delineation of the EOF effect in SDS coated NPs as unlike dsDNA (double-stranded DNA) their total charge is ambiguous and highly SDS dependent.

Herein, we characterized the EOF effect after coating SiN_x NP surfaces with SDS, using (i) dsDNA molecules of various lengths, which are subject to both EP and EOF. (ii) Uncharged analytes (small zwitterion organic dyes) are subject primarily to EOF. Our results demonstrate that when EOF intensity is finely tuned it can lead up to a >30-fold increase in the translocation dwell-times (t_D) of dsDNA, without any deterioration of the NP noise, hence providing key advantages to single-molecule biosensing. Electro-optical measurements of similarly prepared NPs confirmed enhanced physical fluid flow into the NP when the EOF direction was biased in the *cis* to *trans* orientation whereas the EP forces on negatively charged objects were pointing *trans* to *cis*. These results are in line with numerical simulations of the EOF velocity field inside and in the vicinity of the nanopore.

Surfactants such as SDS can be used for self-assembled coating of NPs made in planar membranes to enhance their

Received: March 23, 2023
Revised: April 24, 2023

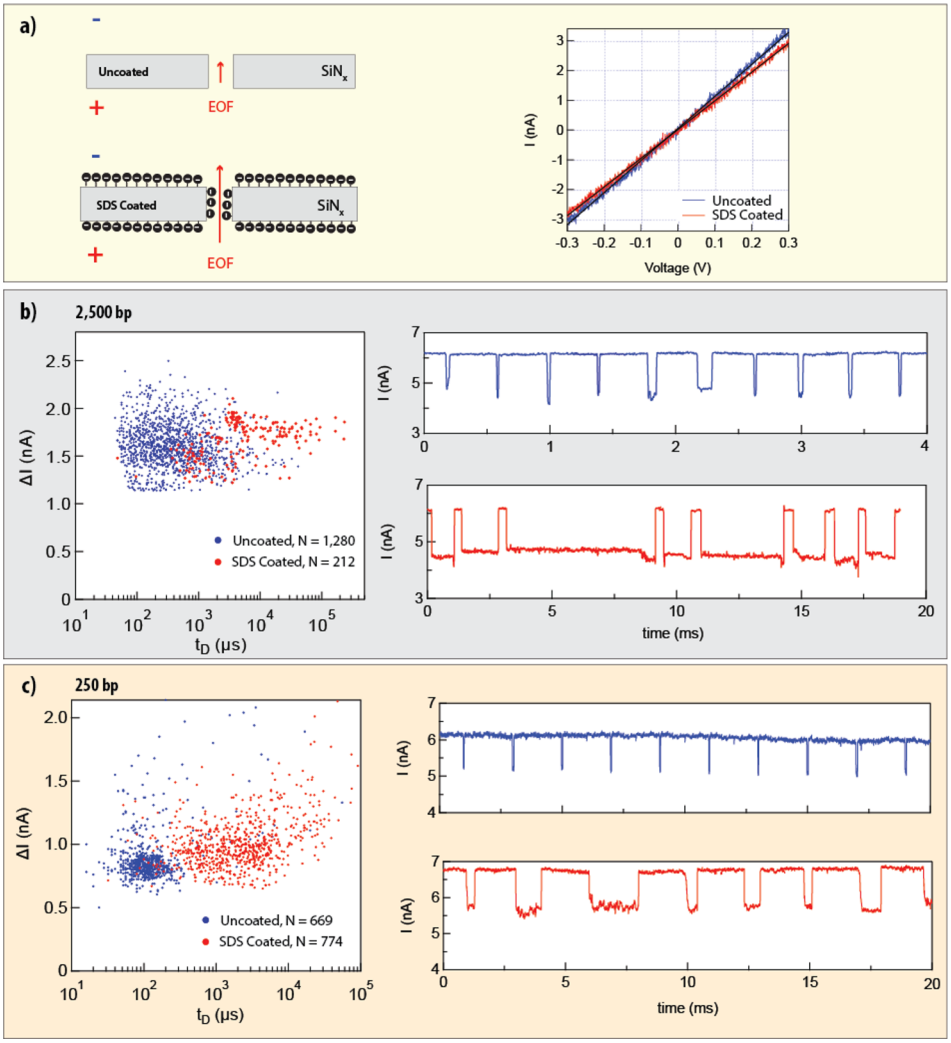

Figure 1. Translocation dynamics of DNA through SDS coated and uncoated sub 5 nm SiN_x nanopore. a) Schematic illustration of the of electro-osmotic flow (EOF) direction through uncoated and SDS coated pore. Right panel shows the corresponding $I-V$ curve measurements of the same uncoated and coated SiN_x nanopore (blue and red, respectively). b) Events diagram, shown as scatterplot, of the event amplitude ($\triangle I$) vs dwell-time (t_d) for 2500 bp DNA molecules translocation. In the right panel typical representative concatenated events observed with uncoated (blue) and SDS coated nanopore (red). c) 250 bp translocations characterization. Left panel displays the scatterplot with SDS coated and uncoated nanopore. Right panel shows typical representative concatenated event observed with uncoated (blue) and SDS coated nanopore (red). In all cases, nanopore open current is between 6 and 7 nA at 500 mV.

stability and functionality.[17−19] Low SDS bulk concentrations, below the salt-adjusted critical micelle concentration (CMC), produce a stable coating of the SiN_x surfaces, hence potentially increasing the NP negative surface charge (Figure 1a).[15] However, a direct measurement of the SDS coating inside ssNPs has been difficult. When the NPs are biased with an electrical potential, an EOF is expected to be produced driven by the Na^+ cations layer next to the NP surfaces. The right panel in Figure 1a shows the current−voltage ($I-V$) response of the same NP right after piranha treatment (Uncoated), and after immersion of the same chip in ∼175 μM SDS, indicating a small reduction in conductance (Figure S1 and supporting text). SDS-coated SiN_x nanopores often exhibit improved stability over time, presumably due to surfactant covering of material defects, in some cases remaining stable >72 h without observing an appreciable change in open pore current (i_O), as shown in Figure S1.

We tested the effect of the SDS coating on the electrophoretic-driven translocation of uniform dsDNA molecules (2500 bp and 250 bp long, see Supporting text). Focusing first on the 2500 bp DNA (Figure 1b), we observe a striking shift in the typical t_D of the event by at least an order of magnitude without an appreciable change in the ion-current blockage amplitude (ΔI) (Figure S2). Concatenated, typical translocation events are shown for the uncoated (blue) and SDS-coated (red) experiments. A similar pattern was observed in another experiment using a shorter DNA strand of 250 bp (Figure 1c), namely over a 10-fold increase in t_D without an appreciable change in ΔI before and after SDS coating.

A detailed analysis of the translocation dynamics is presented in Figure 2. In the left-hand panels, we show the t_D distributions of 2500 bp and 250 bp dsDNAs (Figure 2a and 2b, respectively) performed at V = 500 mV. Where possible, data were fit using the "Drift-Diffusion" model (a solution of Poisson-Plank equation), unless statistics were insufficient, in that case we used an exponential tail-fit to extract the characteristic t_D value.[20] Specifically, for the 2500 bp we observe a shift from 300 ± 12 μs to 4780 ± 520 μs before and

https://doi.org/10.1021/acs.nanolett.3c01096
Nano Lett. XXXX, XXX, XXX−XXX

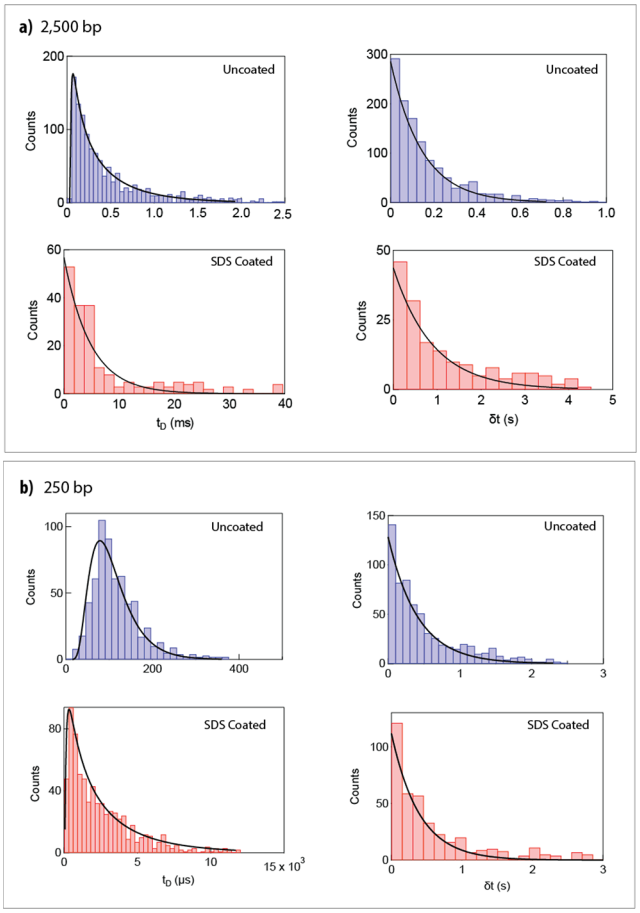

Figure 2. ds-DNA translocation and capture rate dynamics characterization with the SDS coated and uncoated nanopore. a) Left panels shows the dwell time (t_d) histograms for uncoated (blue) and SDS coated (red) nanopore, we observed a 16-fold dwell time increment with SDS coating for 2500 bp translocations. Right panels display the event capture rate (δt) histograms for uncoated (blue) and SDS coated nanopore (red) fitted monoexponentially (black). b) Similarly, 250 bp translocations through a similar nanopore size (12 nS in all cases). Left panels for the dwell time in both conditions; we observed a 34-fold slowing down of translocation speed with the SDS coating. The right panels display the event capture rate (similar color scheme as panel a).

after SDS coating, respectively, or a 16-fold t_D increase. Interestingly, for the shorter 250 bp DNA we observe a typical t_D of 63.4 ± 3.7 μs before coating and 2190 ± 130 μs *after* SDS coating, an enhancement factor of ∼34 (Figure 2b). However, when we compare the events' capture distribution (the rate at which dsDNA arrives and enters the NP) per Molar of the dsDNA, we observe >6-fold reduction for the 2500 events rate (2.28 ± 0.08 and 0.37 ± 0.04 s^{-1} nM^{-1} before and after coating, respectively) as shown in Figure 2a right-hand panels. But for the 250 bp DNA, we observe no change in the events' capture rate before and after coating (2.41 ± 0.16 and 2.54 ± 0.20 s^{-1} nM^{-1}, respectively, Figure 2b right-hand panels). Taken together, SDS-coated NPs exhibit a significant slowing-down of the translocation dynamics without much effect on ssNP performance (the events' mean amplitude and the ion-current RMS noise). In contrast, the events' mean capture rates are differentially affected: longer DNA molecules suffer from a significant reduction in the rate, whereas the shorter DNA strands do not.

Label-free sensing of short dsDNA fragments is highly significant for many biomedical applications.[21,22] For example, cell-free circulating tumor DNA as well as nucleosome DNA are naturally cut into short fragments of ∼150 bp (or less).[23−25] The typical translocation speed of such DNA fragments is at the order of <10 μs,[26] challenging NP sensing as high bandwidth amplifiers involve substantially increased overall noise.[27] The experiments shown in Figure 1 and Figure 2 suggest that slowing down in SDS-coated NP may be achieved *without* compromising NP sensing performances or a reduced capture rate.

To that end, we coated ∼4 nm NPs with SDS as before and measured the translocation dynamics of 100 and 50 bp DNA under V = 500 mV (Figure 3). In experiments using V = 500

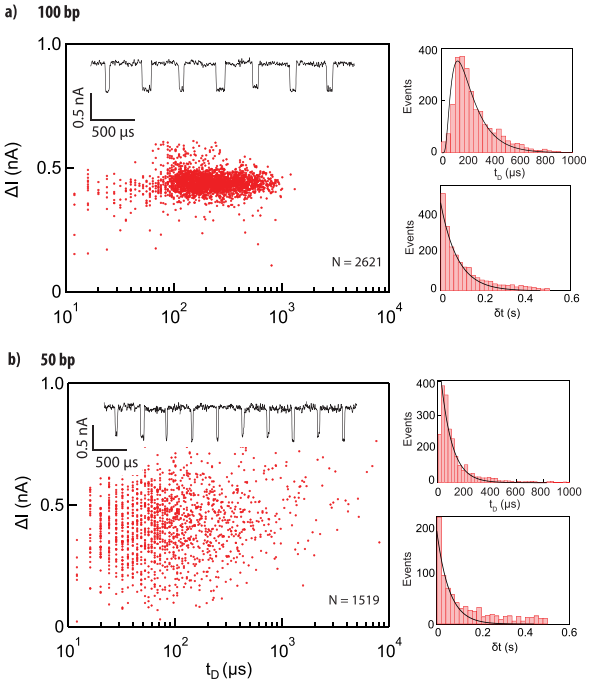

Figure 3. EOF-assisted high sensing resolution measurement of short ds-DNAs. a) Event diagram, shown as a scatterplot, of the event amplitude ($\triangle I$) vs dwell-time (t_d) for 100 bp DNAs translocations; inset shows some concatenated representative events. The two right panels show the dwell time (t_d) histogram and the capture rate (δt) histogram. The obtained fitted values for both parameters are 190 ± 9 μs and 4.23 ± 0.26 nM $^{-1}$ s^{-1} respectively. b) Event diagram, shown as a scatterplot, of the event amplitude ($\triangle I$) vs dwell-time (t_d) for 50 bp DNAs translocations; inset shows some concatenated representative events. The translocation dwell time for 50 bp (85 ± 9 μs) is 2.23 time shorter than 100 bp translocations. However, the event capture rate (5.93 ± 0.78 nM $^{-1}$ s^{-1}) is 1.40 times higher compared with that of the 100 bp translocation.

mV of the uncoated NP, the events were too short for our sensing apparatus. Using a smaller voltage bias of V = 350 mV resulted in a poor capture rate making data collection extremely tedious. In contrast, when using the SDS-coated NP for the 100 bp (Figure 3a) we obtain a typical t_D 190 ± 9 μs (N = 2621) or roughly ∼2 μs per base-pair, and for the 50 bp DNA molecules, we consistently obtain a somewhat broader distribution with a typical t_D 85 ± 9 μs at 500 mV (N = 1519), Figure 3b. The larger scatter of the events amplitude makes sense considering that in this case, the DNA contour length is on-par with the nominal membrane

https://doi.org/10.1021/acs.nanolett.3c01096
Nano Lett. XXXX, XXX, XXX−XXX

thickness. Consistent with our results shown in Figure 2, the events rate did not seem to suffer from the SDS coating allowing us to record translocations at high rates: 4.23 ± 0.26 and 5.93 ± 0.78 nM $^{-1}$ s^{-1}, for the 100 and 50 bp DNA, respectively. We note that in all these cases, we observe >20-fold-slower translocation times as compared with previous reports, without any effect on the NP noise and the events capture rate.[26]

dsDNA is a strong electrolyte, and its translocation dynamics are dominated by both the electrophoretic (EP) forces in the vicinity and inside the NP, as well as EOF. Moreover, both the EP force and the EOF are directly proportional to the same electrical potential gradient and these two forces are therefore coupled. To decouple these two phenomena, and shed light on the results in Figures 1−3, we introduced an electro-optical sensing strategy using uncharged small molecules, as shown in Figure 4a.[28] Electrically neutral fluorescent molecules (Atto 565 or Atto 647) are used here to directly image the effect created by the in-pore EOF (see SI Movies 1 and 2).[29,30] To facilitate optical imaging and reduce the photoluminescent background, we fabricated nanopores in a 2 μm wide well formed in the SiN_x membranes that were locally thinned down to 20 nm nominal thickness.[31] First, we performed simultaneous ion-current and fluorescence measurement of the uncoated NP as a function of the applied voltage as shown schematically in Figure 4a. For an uncoated nanopore, the fluorescence signal is unaffected by the voltage magnitude or polarity (Figure 4b, top panel). A small buildup of fluorescent is observed over time, presumably due to the slight hydrophobicity of the fluorophores.

In contrast, SDS-coated NPs showed a strikingly different behavior: we observe a clear and immediate response of the fluorescence intensity in the pore vicinity to the applied voltage (Figure 4b, lower panel). When the fluorophores are placed in the *cis* chamber, a negative bias to the *trans* chamber produces an increased fluorescent signal with the applied voltage. This phenomenon is reversal: switching the voltage on and off modulates the fluorescent signal, respectively. The increment in the fluorescence intensity strictly signifies a stronger EOF of the fluorophores into the NP. We can rule out the possibility of SDS micelle-dye interaction since the experiment was performed below the CMC.[32] Additionally, we can rule out that possible SDS molecules interacting with the Atto molecules contributed to the in-pore fluorescence signal. These negatively charged complexes (if existed) would be pushed electrophoretically away from the pore further into the *cis* chamber.

An accumulation of the camera images during the time that the voltage is on shows a bright spot at the NP location in the center of the thin region. In contrast, negligible fluorescence appears at the NP location when we add the images while the voltage is off. Both the fluorescence intensity and the ion current (measured simultaneously) show a linear dependence on the applied voltage (Figure 4c), suggesting that the enhancement of fluorescence with negative voltage is due to the EOF, which induces a fluorophore flux through the NP in *cis* to *trans* direction. Given that the fluorophores are neutrally charged (zwitterionic), this provides a direct indication of the EOF in an SDS-coated NP.

The strong electrostatic screening of our salt buffer (0.4 M) promotes the formation of high-density SDS monolayers on the SiN_x surfaces. Given the physical size of the SDS polar head (a sulfur atom surrounded by 4 oxygen atoms), the theoretical dense packing of an SDS monolayer would produce up to ~4 × 10^{18} electron charges per m^2 (−0.7 C/m^2). This is

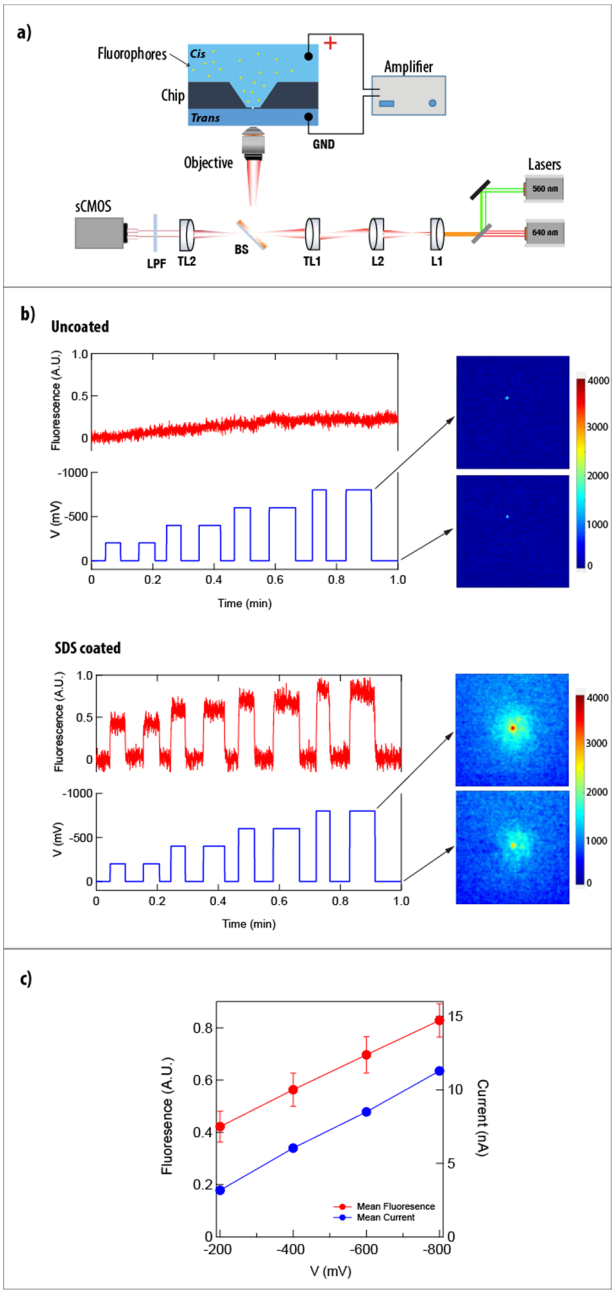

Figure 4. Electro-optical sensing of electro-osmotic flow in SDS coated nanopore. a) Schematic illustration of setup equipped with all the electrical and optical components for the electro-optical measurements. The fluorophores are in the top chamber and generate a fluorescence response when they flow through the nanopore. b) The upper panel shows the uncoated pore response on applying different voltage from −200 to −800 mV. The bottom panel shows the response of the SDS coated nanopore on applying different transmembrane voltages (from −200 to −800 mV). The red synchronous curve with the applied voltage shows that the change in fluorescence intensity is a voltage-driven response. All the heat maps are representing the fluorescence intensity in the nanopore region at 0 and −400 mV respectively. c) The blue points are representing the experimental open pore current at different voltage (14 nS), and the red points are representing the corresponding normalized fluorescence intensities.

https://doi.org/10.1021/acs.nanolett.3c01096
Nano Lett. XXXX, XXX, XXX−XXX

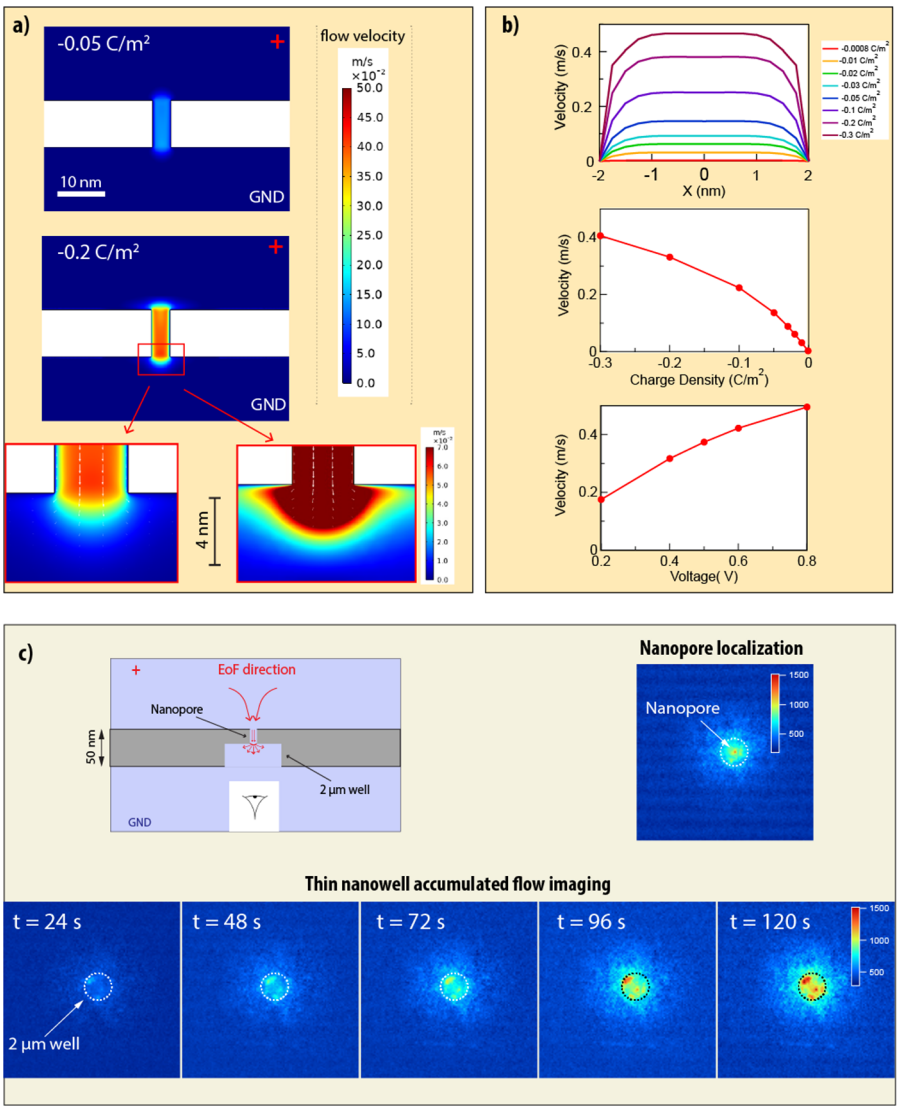

Figure 5. Numerical simulation and single molecule nanopore mapping of the EOF. a) The electro-osmotic flow profile at two different charge densities −0.05C/m^2 and −0.20C/m^2. Clearly, the higher surface charge density exhibits stronger hydro-dynamic flow. b) The upper panel shows the flow profile at the center of the nanopore (r = −2 to 2, Z = 0) at different surface charge densities. The EOF shows an increment with increasing the surface charge density in 4 nm nanopore under a bias condition of 300 mV. The middle panel shows the change in EOF at different charge densities at same bias voltage of 300 mV. The bottom panel show that EOF increases with the increment in the transmembrane voltage at a surface charge density of −0.20 C/m^2. c) The experiment diagram (top left) depicts the flow of a 25 pM fluorophore concentration from the top to bottom of the membrane (arrow direction). The membrane's bottom side has a 10 nm thin section (2 μm in diameter), and the observation point is orthogonal to the EOF (arrows) in the direction of the thin region. Top-right figure clearly illustrates the localized position of the nanopore by summing thousands of frames of fluorophore flow time snaps. The dashed circle indicates the thin region boundaries. Bottom figures (left to right) show the sum of a large number (>1000) of frames in each 2D plot revealing the stagnant points of the flow where the fluorophores get relax and get localized in their time snaps.

an upper-limit estimation, and in practice we expect the SDS monolayer density to be smaller. Nevertheless, it provides a rough value for the maximum surface charge density, and it is in line with recent studies of native (uncoated) the SiN_x NP surface charge at high salt concentrations and normal pH.[33] To check if this level of charge density can produce substantial EOF in a typical ssNP we used finite elements numerical simulation software of the Nernst-Plank equation in 2D to calculate the ions distribution inside and in the vicinity of the NP, simultaneously solved with the Navier−Stokes equation in the entire model, to calculate the velocity field.[34] Based on the estimation of the surface charge, we repeated the numerical calculations in the range of 0 to −0.3 C/m^2 and under the practical experimental voltage range of 0.2 to 0.8 V.

Figure 5a shows two typical magnitudes of the fluid velocity field calculated for surface charge densities of −0.05 and −0.2 C/m^2. In both cases, a 0.3 V potential drop is applied at distances sufficiently far from the NP. When the NP surface charge is increased, we observe a marked rise in the fluid velocity inside the NP, up to typically 0.4 m/s. The line profile of the velocity across the width of the NP shows characteristic EOF "plug-flow" (Figure 4b, top panel) with a nearly uniform velocity in the center area of the pore and vanishing speed at the pore's surfaces, obeying the no-slip conditions applied. The plug maximum velocity amplitudes (at the plateau) grow

https://doi.org/10.1021/acs.nanolett.3c01096
Nano Lett. XXXX, XXX, XXX−XXX

nonlinearly with the absolute value of the surface charge and the applied electrical potential (Figure 4b, middle and lower panels). These results agree with our expectations as they show that the levels of surface charge likely to be induced by the SDS coating can produce strong EOF plug velocities.

The EOF plug velocities (roughly 0.2 m/s) are a direct consequence of the strong electrical field intensity across the thin SiN_x membrane ($\sim 10^7$ V/m). One, however, may ask if this plug flow velocity translates to a sufficiently strong force that can slow-down the DNA translocation. As a rough estimation, we model the DNA as a simple cylinder with a mean diameter a = 2.2 nm, and approximate the hydrodynamic drag force produced by EOF as $F_{EOF} = \xi v_{EOF} = 2\pi\eta v_{EOF}\frac{la}{d-a}$ where d and l are respectively the cylindric nanopore diameter and length, η is the fluid's viscosity and v_{EOF} is the calculated EOF velocity. Plugging in typical NP values (d = 4 nm, l = 20 nm) and a typical fluid velocity of 0.2 m/s, we obtain a EOF drag force contribution $F_{EOF} \approx 20$ pN. This force is on-par with the estimated in-pore Columbic force applied on a dsDNA molecule $F_{EP} \approx 100$ pN. These are crude estimations ignoring other factors affecting DNA translocations (particularly in-pore interactions), but nevertheless they are in line with our experiments showing a significant slowing down due to the EOF.

Another effect of the EOF is the creation of asymmetrical ion concentration fields in the vicinity of the pore: at the positively biased side of the NP an ion-depleted zone is formed (of both the cations and anions), whereas on the grounded ("GND") side, a respective local increase in the ions concentration is observed (Figures S5 and S6). Zooming in to the GND side of the NP side (Figure 1a, bottom panels), we see a steep gradient droping to zero velocity over a distance of ~5 nm, and diverging rapidly from the pore entry. In other words, despite the relatively large in-pore plug velocity its impact outside the pore is limited to distances of the same order of the NP diameter. We hypothesize that this EOF pattern is responsible for the reduced capture rate of the longer dsDNA coil as compared with the short DNAs. The EOF gradient pointing away from the pore may not be strong enough to expel the dsDNA coils away from the NP as the latter is held by the EP forces acting on the full-length DNA charge. However, it is sufficiently strong to disrupt the end-threading process of the semiflexible 2.5 kbp DNA coil ($r_g \sim$ 120 nm).[35] In contrast, shorter DNA strands, and specifically in the case of semiflexible rods (DNA persistent length is roughly 150 bp), can easily align along the EOF lines, essentially minimizing their overall hydrodynamic friction when approaching the NP.[36] This may explain why the shorter dsDNA molecules are captured at similar rates with or without the EOF.

Further mapping of the EOF-driven flow in the vicinity of the pore is made possible using a much lower concentration of a neutrally charged fluorophore ATTO 647 (C = 25 pM). Here, single fluorescent molecules can be imaged in the NP's "thin-region", as discrete fluorescent spots appearing in several consecutive frames in the movies (SI Movie 3). The motion of the fluorophores in and out of the field of view is too fast to allow their trajectory tracing; however, two-dimensional intensity images can be produced by summing >1000 camera frames (Figure 5c). These images show that the fluorophores ejected from the NPs into the 2 μm well, fill the well area in accord with the strong divergence of the EOF lines outside the NP. Moreover, the images show that some immobile fluorophores right at the well walls, presumably due to sticking. When we remove the strong contributions of the three stuck dyes on the well walls, a sharp intensity peak is observed at the center of the well where the NP is formed (Figure 5c, right panel). Overall, these measurements strengthen the interpretation that EOF flow lines outside the NP diverge at all possible directions and rapidly vanish outside the NP.

In summary, besides the basic importance of understanding the in-pore anionic surfactant coating and the resulting EOF in small planar NPs (<5 nm), it is highly relevant for many emerging biomedical sensing applications, from circulating tumor DNAs sensing to short peptides. Here we investigated DNA translocations through the SDS-treated NPs, showing >30-fold increase in the DNA translocation dwell-time when comparing with an "uncoated" nanopore. Importantly, the SDS treatment has not compromised the NPs noise, as compared with the uncoated nanopores. We hypothesize that the main factor contributing to the slowing down is the in-pore EOF associated with the negative surface charge of the SDS-coated nanopores.

To check our hypothesis, we introduced electro-optical sensing of the NP system, in which the ion current and the 2D fluorescence images were simultaneously acquired. By using neutrally charged fluorophores, we decoupled the EP effect from EOF. Our results show that the SDS coating likely responsible for strong in-pore EOF medicated by the Na^+ ions. Moreover, the electro-optical measurement could inform us of the EOF flow pattern in the vicinity of the NP, helping to explain why short DNA molecules are efficiently captured by the NP as compared with longer DNAs. Our experimental results offer important practical benefits allowing simple high sensitivity sensing of small dsDNA (50 bp) and a high DNA capture rate with no loss in SNR. The SDS coating opens up many new avenues in the nanopore sensing field specifically for the emerging single-molecule protein sequencing technology.[37]

■ ASSOCIATED CONTENT

Supporting Information

The Supporting Information is available free of charge at https://pubs.acs.org/doi/10.1021/acs.nanolett.3c01096.

Description of the nanopore fabrication and device assembly, sample preparation for nanopore experiments, optical setup and data acquisition, data acquisition and analysis for electrical only measurement, data acquisition and analysis for electrical-optical measurement, finite element numerical simulations (PDF)

SI Movie 1: Synchronous Electro-optical flow in SDS coated nanopore at different voltage (MP4)

SI Movie 2: Electro-optical flow in Uncoated nanopore at different voltage (MP4)

SI Movie 3: Single fluorophore flow and nanopore mapping (MP4)

■ AUTHOR INFORMATION

Corresponding Author

Amit Meller − *Russell Berrie Nanotechnology Institute, Technion IIT, Haifa 3200003, Israel; Department of Biomedical Engineering, Technion IIT, Haifa 3200003, Israel;* orcid.org/0000-0001-7082-0985; Email: ameller@technion.ac.il

https://doi.org/10.1021/acs.nanolett.3c01096
Nano Lett. XXXX, XXX, XXX−XXX

Authors

Neeraj Soni − *Russell Berrie Nanotechnology Institute, Technion IIT, Haifa 3200003, Israel; Department of Biomedical Engineering, Technion IIT, Haifa 3200003, Israel*

Navneet Chandra Verma − *Department of Biomedical Engineering, Technion IIT, Haifa 3200003, Israel*

Noam Talor − *Department of Biomedical Engineering, Technion IIT, Haifa 3200003, Israel*

Complete contact information is available at: https://pubs.acs.org/10.1021/acs.nanolett.3c01096

Author Contributions

#N.S. and N.C.V. contributed equally. N.S., N.C.V., and N.T. jointly performed all nanopore measurements and analyzed the data. A.M. designed and supervised the research. All authors cowrote the manuscript.

Notes

The authors declare no competing financial interest.

■ ACKNOWLEDGMENTS

We thank Dr. Yulia Marom for assistance in the fabrication of nanopore devices, and Dr. Moran Bercovici for kind advise related to the numerical simulations. This project has received funding from the European Research Council (ERC) No. 833399 (NanoProt-ID) under the European Union's Horizon 2020 research and innovation programme grant agreements and from the IIA award "Liquid-Bx". N.C.V. has been supported in part at the Technion by a fellowship of the Israel Academy of Science and Humanities and Israel Council for Higher Education.

■ REFERENCES

(1) Deamer, D.; Akeson, M.; Branton, D. Three Decades of Nanopore Sequencing. *Nat. Biotechnol.* **2016**, *34* (5), 518−524.

(2) Xue, L.; Yamazaki, H.; Ren, R.; Wanunu, M.; Ivanov, A. P.; Edel, J. B. Solid-State Nanopore Sensors. *Nat. Rev. Mater.* **2020**, *5* (12), 931−951.

(3) Ying, Y. L.; Hu, Z. L.; Zhang, S.; Qing, Y.; Fragasso, A.; Maglia, G.; Meller, A.; Bayley, H.; Dekker, C.; Long, Y. T. Nanopore-Based Technologies beyond DNA Sequencing. *Nat. Nanotechnol.* **2022**, *17* (11), 1136−1146.

(4) Wanunu, M.; Sutin, J.; McNally, B.; Chow, A.; Meller, A. DNA Translocation Governed by Interactions with Solid-State Nanopores. *Biophys. J.* **2008**, *95* (10), 4716−4725.

(5) Haywood, D. G.; Saha-Shah, A.; Baker, L. A.; Jacobson, S. C. Fundamental Studies of Nanofluidics: Nanopores, Nanochannels, and Nanopipets. *Anal. Chem.* **2015**, *87* (1), 172−187.

(6) Schmid, S.; Stömmer, P.; Dietz, H.; Dekker, C. Nanopore Electro-Osmotic Trap for the Label-Free Study of Single Proteins and Their Conformations. *Nat. Nanotechnol.* **2021**, *16* (11), 1244−1250.

(7) Huang, G.; Willems, K.; Soskine, M.; Wloka, C.; Maglia, G. Electro-Osmotic Capture and Ionic Discrimination of Peptide and Protein Biomarkers with FraC Nanopores. *Nat. Commun.* **2017**, *8* (1), 1−11.

(8) Bayley, H.; Braha, O.; Gu, L. Q. Stochastic Sensing with Protein Pores. *Adv. Mater.* **2000**, *12* (2), 139−142.

(9) Chinappi, M.; Yamaji, M.; Kawano, R.; Cecconi, F. Analytical Model for Particle Capture in Nanopores Elucidates Competition among Electrophoresis, Electroosmosis, and Dielectrophoresis. *ACS Nano* **2020**, *14* (11), 15816−15828.

(10) Laohakunakorn, N.; Thacker, V. V.; Muthukumar, M.; Keyser, U. F. Electroosmotic Flow Reversal Outside Glass Nanopores. *Nano Lett.* **2015**, *15* (1), 695−702.

(11) Laohakunakorn, N.; Gollnick, B.; Moreno-Herrero, F.; Aarts, D. G. A. L.; Dullens, R. P. A.; Ghosal, S.; Keyser, U. F. A Landau-Squire Nanojet. *Nano Lett.* **2013**, *13* (11), 5141−5146.

(12) Shi, X.; Pumm, A. K.; Isensee, J.; Zhao, W.; Verschueren, D.; Martin-Gonzalez, A.; Golestanian, R.; Dietz, H.; Dekker, C. Sustained Unidirectional Rotation of a Self-Organized DNA Rotor on a Nanopore. *Nat. Phys.* **2022**, *18* (9), 1105−1111.

(13) Di Fiori, N.; Squires, A.; Bar, D.; Gilboa, T.; Moustakas, T. D.; Meller, A. Optoelectronic Control of Surface Charge and Translocation Dynamics in Solid-State Nanopores. *Nat. Nanotechnol.* **2013**, *8* (12), 946−951.

(14) Anderson, B. N.; Muthukumar, M.; Meller, A. PH Tuning of DNA Translocation Time through Organically Functionalized Nanopores. *ACS Nano* **2013**, *7* (2), 1408−1414.

(15) Soni, N.; Freundlich, N.; Ohayon, S.; Huttner, D.; Meller, A. Single-File Translocation Dynamics of SDS-Denatured, Whole Proteins through Sub-5 Nm Solid-State Nanopores. *ACS Nano* **2022**, *16* (7), 11405−11414.

(16) Restrepo-Pérez, L.; John, S.; Aksimentiev, A.; Joo, C.; Dekker, C. SDS-Assisted Protein Transport through Solid-State Nanopores. *Nanoscale* **2017**, *9* (32), 11685−11693.

(17) Yusko, E. C.; Johnson, J. M.; Majd, S.; Prangkio, P.; Rollings, R. C.; Li, J.; Yang, J.; Mayer, M. Controlling Protein Translocation through Nanopores with Bio-Inspired Fluid Walls. *Nat. Nanotechnol.* **2011**, *6* (4), 253−260.

(18) Eggenberger, O. M.; Ying, C.; Mayer, M. Surface Coatings for Solid-State Nanopores. *Nanoscale* **2019**, *11* (42), 19636−19657.

(19) Eggenberger, O. M.; Leriche, G.; Koyanagi, T.; Ying, C.; Houghtaling, J.; Schroeder, T. B. H.; Yang, J.; Li, J.; Hall, A.; Mayer, M. Fluid Surface Coatings for Solid-State Nanopores: Comparison of Phospholipid Bilayers and Archaea-Inspired Lipid Monolayers. *Nanotechnology* **2019**, *30* (32), 325504.

(20) Li, J.; Talaga, D. S. The Distribution of DNA Translocation Times in Solid-State Nanopores. *J. Phys.: Condens. Matter* **2010**, *22* (45), 454129.

(21) van Kooten, X. F.; Rozevsky, Y.; Marom, Y.; Ben Sadeh, E.; Meller, A. Purely Electrical SARS-CoV-2 Sensing Based on Single-Molecule Counting. *Nanoscale* **2022**, *14* (13), 4977−4986.

(22) Rozevsky, Y.; Gilboa, T.; Van Kooten, X. F.; Kobelt, D.; Huttner, D.; Stein, U.; Meller, A. Quantification of MRNA Expression Using Single-Molecule Nanopore Sensing. *ACS Nano* **2020**, *14* (10), 13964−13974.

(23) Wanunu, M.; Dadosh, T.; Ray, V.; Jin, J.; McReynolds, L.; Drndić, M. Rapid Electronic Detection of Probe-Specific MicroRNAs Using Thin Nanopore Sensors. *Nat. Nanotechnol.* **2010**, *5* (11), 807−814.

(24) Wang, Y.; Zheng, D.; Tan, Q.; Wang, M. X.; Gu, L. Q. Nanopore-Based Detection of Circulating MicroRNAs in Lung Cancer Patients. *Nat. Nanotechnol.* **2011**, *6* (10), 668−674.

(25) Marcozzi, A.; Jager, M.; Elferink, M.; Straver, R.; van Ginkel, J. H.; Peltenburg, B.; Chen, L. T.; Renkens, I.; van Kuik, J.; Terhaard, C.; de Bree, R.; Devriese, L. A.; Willems, S. M.; Kloosterman, W. P.; de Ridder, J. Accurate Detection of Circulating Tumor DNA Using Nanopore Consensus Sequencing. *npj Genomic Med.* **2021**, *6* (1), 1−11.

(26) Venkatesan, B. M.; Bashir, R. Nanopore Sensors for Nucleic Acid Analysis. *Nat. Nanotechnol.* **2011**, *6* (10), 615−624.

(27) Lin, C. Y.; Fotis, R.; Xia, Z.; Kavetsky, K.; Chou, Y. C.; Niedzwiecki, D. J.; Biondi, M.; Thei, F.; Drndić, M. Ultrafast Polymer Dynamics through a Nanopore. *Nano Lett.* **2022**, *22* (21), 8719−8727.

(28) Gilboa, T.; Meller, A. Optical Sensing and Analyte Manipulation in Solid-State Nanopores. *Analyst* **2015**, *140* (14), 4733−4747.

(29) Product Information for ATTO 647. https://www.atto-tec.com/ATTO-647.html (accessed Feb 15, 2023).

(30) Product Information for ATTO 565. https://www.atto-tec.com/fileadmin/user_upload/Katalog_Flyer_Support/ATTO_565.pdf (accessed Feb 15, 2023).

(31) Zrehen, A.; Gilboa, T.; Meller, A. Real-Time Visualization and Sub-Diffraction Limit Localization of Nanometer-Scale Pore Formation by Dielectric Breakdown. *Nanoscale* **2017**, *9* (42), 16437−16445.
(32) Zhang, X.; Poniewierski, A.; Jelińska, A.; Zagozdzon, A.; Wisniewska, A.; Hou, S.; Hołyst, R. Determination of Equilibrium and Rate Constants for Complex Formation by Fluorescence Correlation Spectroscopy Supplemented by Dynamic Light Scattering and Taylor Dispersion Analysis. *Soft Matter* **2016**, *12* (39), 8186−8194.
(33) Lin, K.; Li, Z.; Tao, Y.; Li, K.; Yang, H.; Ma, J.; Li, T.; Sha, J.; Chen, Y. Surface Charge Density Inside a Silicon Nitride Nanopore. *Langmuir* **2021**, *37* (35), 10521−10528.
(34) Mao, M.; Sherwood, J. D.; Ghosal, S. Electro-Osmotic Flow through a Nanopore. *J. Fluid Mech.* **2014**, *749*, 167−183.
(35) Tree, D. R.; Muralidhar, A.; Doyle, P. S.; Dorfman, K. D. Is DNA a Good Model Polymer? *Macromolecules* **2013**, *46* (20), 8369−8382.
(36) Ermann, N.; Hanikel, N.; Wang, V.; Chen, K.; Weckman, N. E.; Keyser, U. F. Promoting Single-File DNA Translocations through Nanopores Using Electro-Osmotic Flow. *J. Chem. Phys.* **2018**, *149* (16), 163311.
(37) Alfaro, J. A.; Bohländer, P.; Dai, M.; Filius, M.; Howard, C. J.; van Kooten, X. F.; Ohayon, S.; Pomorski, A.; Schmid, S.; Aksimentiev, A.; Anslyn, E. V.; Bedran, G.; Cao, C.; Chinappi, M.; Coyaud, E.; Dekker, C.; Dittmar, G.; Drachman, N.; Eelkema, R.; Goodlett, D.; Hentz, S.; Kalathiya, U.; Kelleher, N. L.; Kelly, R. T.; Kelman, Z.; Kim, S. H.; Kuster, B.; Rodriguez-Larrea, D.; Lindsay, S.; Maglia, G.; Marcotte, E. M.; Marino, J. P.; Masselon, C.; Mayer, M.; Samaras, P.; Sarthak, K.; Sepiashvili, L.; Stein, D.; Wanunu, M.; Wilhelm, M.; Yin, P.; Meller, A.; Joo, C. The Emerging Landscape of Single-Molecule Protein Sequencing Technologies. *Nat. Methods* **2021**, *18* (6), 604−617.

https://doi.org/10.1021/acs.nanolett.3c01096
Nano Lett. XXXX, XXX, XXX−XXX